LIGAND-FRAMEWORK COUPLING VIBRATIONS. THE $^2E_g \rightarrow {}^4A_{2g}$ TRANSITION IN THE $Cr(CN)_6^{3-}$ COMPLEX ION

R. Acevedo[a], M. Passman[b] and G. Navarro[c]

[a]Facultad de Ciencias Físicas y Matemáticas, Universidad de Chile
Beaucheff 850, Casilla, 2777, Santiago, Chile
[b]Laser Laboratory, School of Biology and Chemical Sciences
Birkbeck College, University of London
Gordon House, 29, Gordon Square, London, WC1H-0PP, UK
[c]Comisión Chilena de Energía Nuclear, Amunátegui 95, Casilla, 188-D, Santiago, Chile

(Received April 20, 2000; revised version December 27, 2000)

In this research paper we examine the role played by the bending vibrational modes of motion, δ(Cr–C–N) to influence the observed overall and relative vibronic intensity distribution for the $^2E_g \rightarrow {}^4A_{2g}$ phosphorescence of the $Cr(CN)_6^{3-}$ complex ion. The calculation was carried out assuming both: (a) a seven-atom system model (molecular approximation) and (b) a negligible distortion from the octahedral symmetry for the system. The ligand polarization formalism was employed with reference to this system, since the ligand subsystems $(CN)^{-1}$ are highly polarizable and as a consequence a conventional crystal field calculation would be both unrealistic and unappropriate. This system was chosen since there is a solid evidence to conclude that vibrations of the same type in the τ_{1u} and τ_{2u} symmetry blocks induce comparable intensity. This is a clear indication that both the τ_{1u} and τ_{2u}: δ(Cr–C–N) bending vibrations are exceptionally efficient to promote this radiative transition. This dynamical model is tested against the experimental data and it is shown that the model calculation, though approximate, gives results in excellent agreement with experiment.

PACS numbers: 32.70.Fw, 32.70.Cs

1. Introduction

The $^2E_g \rightarrow {}^4A_{2g}$ polarized luminescence spectrum of the $Cr(CN)_6^{3-}$ complex ion in a single crystal of the four layered orthorhombic polytype of $K_2Co(CN)_6$ have been measured at temperatures of 5 K and above by Flint and co-workers [1–3].

This phosphorescence is exceptionally strong and well resolved and over 11 lines may be observed in the spectrum. The allowed excited ^2E_g of this complex ion is split however, by approximately 49 cm^{-1} due to both spin–orbit coupling and the low site symmetry (C_i), but at 5 K just the lower of these states is populated. In the current work and for the sake of simplicity we shall neglect the distortion giving rises to the group–subgroup chain $SO_3 \supset O_h \supset O \supset \ldots \supset S_2 = C_i \supset C_1$, then we will assume that the Cr^{3+} occupies sites of octahedral symmetry. This is indeed a crude approximation to adopt since the experimental evidence is clear to show a degree of distortion. Several studies on the crystal structure for the $K_2Co(CN)_6$ system have been performed by several authors [4–10]. More recently, Artman et al. [9] reported the $K_2Co(CN)_6$ is polytypic with two unit cells predominating (one orthorhombic and the other monoclinic).

The monoclinic space group is that reported earlier $P2_1c(C_{2h}^5)$, while the orthorhombic unit cell is currently somewhat more prevalent [9] and falls in the space group $Pnca(D_{2h}^{14})$. The resulting unit cell groups may be correlated to the $Co(CN)_6^{-3}$ site group and the isolated ion group (O_h), by employing standard correlation tables. It is interesting to observe that for the monoclinic structure, the site group is $C_i = S_2$, while for the orthorhombic structure the site group is C_2. In the former case, the unit cell group is C_{2h}, while in the latter case the unit cell group is D_{2h}.

For the monoclinic structure, since the site group is C_i and all the odd parity vibrations of the isolated ion group (O_h) are infrared active (α_u), it follows that the even parity vibrational modes of the isolated ion group will be infrared inactive (α_g). Besides, under the unit cell group C_{2h}, the isolated ion's vibrations τ_{1u} and τ_{2u} will each split into three components, one of them polarized along the z-axis and the other two being polarized in the xy-plane. Furthermore, under the D_{2h} unit cell group, all the vibrations of the isolated ion have an infrared active component. For instance, the α_{1g} and the ε_g vibrations of the isolated complex ion will have an infrared active component polarized only along the z-axis. All other vibrations of the complex ion have three infrared active components and they are polarized along each of the three crystal axes.

Bearing in mind these selection rules and the assumptions involved on the choice of a molecular model (an octahedral site symmetry with the neglect of the descent of symmetry), we have (in the first-order approximation) attempted a vibronic calculation for the $^2E_g \to {}^4A_{2g}$ phosphorescence. Additionally and in order to justify the use of a molecular model, we have neglected the coupling among the internal and external vibrations. We will perform a ligand polarization calculation to estimate both the total and the relative vibronic intensity distributions due to the odd parity vibrational modes, based upon the highly polarizable character of the ligand subsystems CN^{1-}. To perform a complete calculation, including the crystal field contribution to the total transition dipole moment, major changes and sophistication should be included in our model calculation. Firstly, a reliable set of atomic charges should become available. Secondly, the motion of the ligand lone pair, out of the internuclear axis Cr–C should be included explicitly (the symmetry coordinates should be modified so that to include the ligand lone pair motion). Finally, a full lattice dynamic calculation in the proper symmetry space group should be carried out. This is indeed a major task, and as far as we know the experimental data available for this system is both limited and scarce. At this stage, we have decided to use a simple model based upon the experimental data available for this system so that to study the role played, in the intensity mechanism, by the ligand subsystems-framework coupling vibrations.

There has been an extensive discussion in the literature about the role played by the ligand subsystems, the framework, the coupling among the ligands, and the framework vibrations in the intensity mechanism for vibronically allowed electronic transitions in coordination compounds of the transition metal ions [17–25]. Also, a particular and very interesting discussion has been attached to the role played by the ligand lone pair to the intensities observed in the spectra of a series of coordination compounds of the type $Cr(NH_3)_6^{3+}$, $Ni(NH_3)_6^{2+}$, $Cr(CN)_6^{3-}$, etc. For all these complex ions, the ligand motions out of the internuclear axis, particularly when bending and/or a rocking vibration takes place, seem to be a rather important idea to rationalize the observed vibronic intensities [22, 26].

It is also important to mention a few words about the substantial amount of work done for the $f \rightarrow f$, electronic transitions in the lanthanide type systems. A relevant piece of work, regarding the role played by the internal ligand vibrations (ligand subsystem vibrational modes of motion) as far as the vibronic intensity mechanisms are concerned for these kinds of crystals may be found in Ref. [27]. The main purpose of the work carried out by Stręk and Sztucki [27] was to derive novel expressions for the amplitudes of vibronic transitions combined with the internal ligand vibrations. They found that the second-order theory fails to explain the presence of high-energy phonon side bands related to these vibrations. The nonvanishing terms are derived from third-order perturbation calculations. This suggests that the vibronic lines associated with ligand vibrations should be weak. A good experimental evidence can be found in a classic paper by Flint and Greenough [1], who found that in a series of Cr(III) complexes in octahedral symmetry, the ligand modes involving vibronic origins are two or three orders of magnitudes weaker than the metal-bond-involving vibronic. Nevertheless, the results provided by Flint and Greenough are in contrast with that of Berry et al. [28] for $Eu(AP)_6X_3$ type systems, where strong ligand-mode-involving vibronic lines were observed. Also, similar observations of strong vibronic were obtained for Eu^{3+} in $LaVO_4$ [8]. In this latter case, it has been shown that the mechanism of vibronic transitions in these systems should be associated with the creation of Ln^{3+} pairs. Thus, the reader can find several examples regarding both pure framework and ligand subsystem vibrations, so that a careful and detailed study of the role played by the coupling among the framework-ligand subsystem vibrations is needed to advance the state of the art in this field of research.

2. Preliminary remarks

Within the framework of the ligand polarization model [17, 26, 29, 30], it is essential to know the perpendicular and the parallel components of the polarizability second rank tensor for the ligand subsystems. It is important to have a good estimate of the values of the different fragments of the molecule, such as atoms, bonds, and functional groups. A view that has prevailed for quite sometime is that the polarizability of a molecular system is additive in character, that is the sum of the polarizabilities of the parts [11]. This is based upon the finding that the molar refraction which is proportional to the molecular polarizability is an additive property, that is the various atoms and functional groups in a given molecule may be assigned refraction values whose sum over the whole molecule is the molar refraction and therefore the value for a given group or atom is fairly constant for a variety of molecules. Extensive tabulations of additive atom and group refractions are available in the literature [11, 12]. The additivity hypothesis has been extended to provide polarizability values for various bonds and functional groups [13, 14]. Thus polarizability tensors have been ascribed to various bonds and functional groups according to the hypothesis that component wise addition of the group tensor gives rise to the molecular polarizability tensor. Nevertheless, the additivity hypothesis may be criticized on the grounds that it neglects the interaction among the group in a molecule, for instance those that derive from the electric field are still unclear.

It was the failure of these various optical rotation calculations that led to a re-examination of the validity of additive values for the polarizabilities of atoms. In the atom–dipole interaction model [15] for the polarizability of atoms, the molecule is regarded as a rigid arrangement of N-units each of which has a polarizability concentrated at a particular point in the space. The particular atoms are taken as "units" and their polarizabilities are taken as being placed at the nuclei. If the polarizability of the i-th unit is α_i, then the induced dipole moment μ_i in the i-th unit, to a first-order correction is as follows:

$$\mu_i = \alpha_i \left(E_i - \sum_{j=1 (j \neq i)} T_{ij} \mu_j \right), \tag{1}$$

where E_i is the applied electric field at the i-th unit and T_{ij} is the dipole field tensor whose matrix representation is

$$T_{ij} = -\frac{3}{r_{ij}^5} \begin{bmatrix} x_i x_j - \frac{1}{3} r_{ij}^2 & x_i y_j & x_i z_j \\ y_i x_j & y_i y_j - \frac{1}{3} r_{ij}^2 & y_i z_j \\ z_i x_j & z_i y_j & z_i z_j - \frac{1}{3} r_{ij}^2 \end{bmatrix}, \tag{2}$$

where r_{ij} represents the distance among the i-th and the j-th units and x, y, and z are the components of a vector from the i-th to the j-th unit in Cartesian coordinates (reference frame with respect to the molecule). Also in Eq. (1), on the right-hand side of this equation, the quantity in brackets represents the total electric field at the i-th unit and has taken into account the applied field and the field due to all the other induced dipoles. Also, effects due to residual (permanent) electric dipoles have not been taken into account as they are not expected to affect the net induced moment by the external field.

Thus, Eq. (1) may be written in matrix notations as given below

$$\tilde{A}\mu = E, \tag{3}$$

where $\tilde{A}$ is a $3N \times 3N$ matrix, and μ and E are the corresponding $3N \times 1$ column vectors. Next, let us define $B = A^{-1}$ and obtain the identity

$$\mu = BE \tag{4}$$

and therefore, we obtain

$$\mu_i = \sum_{j=1}^{N} B_{ij} E_j. \tag{5.1}$$

Next, if the molecule is placed in a uniform field, then $E_j = E$, for all j-values, and Eq. (5.1) becomes

$$\mu_i = \sum_{j=1}^{N} B_{ij} E \tag{5.2}$$

and the total induced moment in the molecule, is then given by the identity

$$\mu_{\mathrm{mol}} = \sum_{i=1}^{N} \mu_i = \sum_{i=1}^{N} \sum_{j=1}^{N} B_{ij} E \tag{5.3}$$

and therefore, the polarizability tensor becomes

$$\alpha_{\mathrm{mol}} = \sum_{i=1}^{N} \sum_{j=1}^{N} B_{ij}. \tag{5.4}$$

In the case of a diatomic molecule of the AB type, whose isolated atom polarizabilities are α_{A} and α_{B}, the diagonal form of the α_{mol} has two components $\alpha_{\|}$ and $\alpha_{\perp}$, parallel and perpendicular to the bond axis, respectively. It is straightforward to show that the following identities hold:

$$\alpha_{\|} = \frac{\left(\alpha_{\mathrm{A}} + \alpha_{\mathrm{B}} + 4\frac{\alpha_{\mathrm{A}}\alpha_{\mathrm{B}}}{r^3}\right)}{\left(1 - 4\frac{\alpha_{\mathrm{A}}\alpha_{\mathrm{B}}}{r^6}\right)} \tag{6.1}$$

and

$$\alpha_{\perp} = \frac{\left(\alpha_{\mathrm{A}} + \alpha_{\mathrm{B}} - 2\frac{\alpha_{\mathrm{A}}\alpha_{\mathrm{B}}}{r^3}\right)}{\left(1 - \frac{\alpha_{\mathrm{A}}\alpha_{\mathrm{B}}}{r^6}\right)}. \tag{6.2}$$

Here r stands for the bond distance A–B. Therefore, for a heteronuclear diatomic molecule, this molecular identity becomes anisotropic even though the atoms A and B are isotropic. The predicted polarizability, furthermore of a molecule parallel to its long axis is generally greater than the perpendicular one and deviations from the additivity of the polarizabilities will become large so long as the atomic polarizabilities approach r^3. In Ref. [15] the authors list the polarizability values for a number of atoms in several polyatomic molecules at the sodium line D line (5.894 Å). It follows that the atom polarizability values within the assumption of the additive model are greater than those of the atom dipole interaction model. It is important to refer the reader to Ref. [15], where several inadequacies of the additive model are fully discussed.

Bridge and Buckingham [16] examined the polarization of laser light scattered by gases and illustrated that the depolarization ratio was determined by the anisotropy k of the molecular polarizability tensor. They define

$$k^2 = \frac{(\alpha_{11} - \alpha)^2 + (\alpha_{22} - \alpha)^2 + (\alpha_{33} - \alpha)^2}{6\alpha^2}. \tag{7}$$

Here α_{11}, α_{22}, and α_{33} are the principal polarizabilities of the molecule and α stands for the mean polarizability value, given by

$$\alpha = \frac{1}{3}(\alpha_{11} + \alpha_{22} + \alpha_{33}). \tag{8}$$

The above magnitudes are functions of the frequency of the incident light. For a linear or symmetric top type molecule, Eq. (7) may still be simplified further to give

$$k = \frac{(\alpha_{\|} - \alpha_{\perp})}{3\alpha}. \tag{9}$$

Since the mean polarizability can be determined from the refractive index of a gas, the measurements of the depolarization ratio determines the magnitude of the anisotropic component of the ligand polarizability tensor, defined as $\beta\alpha = \alpha_{\|} - \alpha_{\perp}$. In current experiments, the orientation of the gas molecules is measured through birefringence proportional to $\beta\alpha$. These authors [16] measured the depolarization ratio and derived polarizability anisotropies for the 6.328 Å line, for a series of diatomic and polyatomic molecules. These values are not available for the CN^{-1} subsystem ligands, and therefore a calculation based upon the atom–dipole interaction model is needed.

In the current research work, two models were considered in calculating polarizabilities. Firstly, the CN groups were treated as a diatomic molecule and finally, the polarizability eigenvalues were derived from the experimental data for the CH_3CN molecule [15]. For the former case, the calculated values are $\alpha_{\|} = 1.6099$ Å^3 and $\alpha_{\perp} = 1.0087$ Å^3. Therefore, for $\alpha_{\mathrm{C}} = 0.700$ Å^3, $\alpha_{\mathrm{N}} = 0.450$ Å^3, $\beta\alpha = 0.6003$ Å^3, $\alpha = 1.210$ Å^3 and $k = 0.1664$.

Besides, we repeated the calculation for the CH_3CN [15], and our best fit was achieved for $\alpha_{\|} = 4.8833$ Å^3 and $\alpha_{\perp} = 2.100$ Å^3. These gave rise to similar values as those of the diatomic model system, reported in this section. The values for CO have been reported by Bridge and Buckingham [16] to give $\alpha = 1.970$ Å^3, $\beta\alpha = 0.530$ Å^3 and $k = 0.089$, whereas the calculated values using the current atom−dipole interaction model [15] give: $\alpha = 1.7677$ Å^3, $\beta\alpha = 0.7786$ Å^3 and $k = 0.1468$. (The atom polarizability values used are as follows: $\alpha_{\mathrm{C}} = 0.615$ Å^3 and $\alpha_{\mathrm{O}} = 0.434$ Å^3 [15].) This simple calculation provides a fairly good support for the calculated polarizability values for the molecular fragment CN. In this agreement, we recognize that the values for the second rank tensor components depend on both the wavelength of the incident light and the chemical environment.

3. The coupling among the ligand-framework vibrations

3.1. The transition dipole moment in the ligand polarization formalism

Within the independent system model (ISM), the first-order correction, in the basis of nuclear Cartesian displacement coordinates s_L and s_M, to the vibronic operator is currently written as given below [17, 19, 20, 30]

$$H_{LP}^{(1)} = \sum_L (s_L - s_M)\nabla_L \left[\sum_{k_1,q_1} D_{q_1}^{k_1}(M) \sum_{\alpha=x,y,z} G_{k_1q_1,\alpha}^{LP}(L)\mu^\alpha(L)\right]$$
$$= \sum_L (s_L - s_M) \sum_{k_1,q_1} D_{q_1}^{k_1}(M) \sum_{\alpha=x,y,z} [\nabla_L G_{k_1q_1,\alpha}^{LP}(L)]\mu^\alpha(L). \tag{10}$$

In the above identity, the geometrical dependence of the interaction among the central metal and the transient induced ligand dipoles is afforded by the ligand polarization geometrical factors $G_{k_1q_1,\alpha}^{LP}(L)$, which have been tabulated by Acevedo et al. [30].

Thus, the β-th component to the transition dipole moment associated with the $|0\rangle \to |a\rangle$ is given by the general identity [17, 19]

$$\mu_{0\to a}^\beta = -\sum_{l\neq 0} \frac{2E_l}{E_l^2 - E_a^2} \sum_L (s_L - s_M) \sum_{k_1,q_1} \langle M_0|D_{q_1}^{k_1}(M)|M_a\rangle$$
$$\times \sum_{\delta=x,y,z} [\nabla_L G_{k_1q_1,\delta}^{LP}(L)]\mu_{0l}^\beta \mu_{0l}^\delta. \tag{11}$$

In the above identity, the transient induced ligand dipoles μ^β and μ^δ refer to the β-th and the α-th polarization directions in the complex molecule based on a coordinate frame with the metal ion centered at the origin.

Generally speaking, the symmetry axis of a cylindrically symmetric ligand (the cylinder axis) has an orientation neither parallel nor perpendicular to the principal coordinate frame of the metal complex as a whole (x, y, z). It is very often necessary to resolve the induced ligand dipoles μ^β and μ^δ vectors referring to the (x, y, z) frame into components referring to the (x', y', z') frame of the particular ligand subsystem. For our purposes, we shall regard the CN groups to be cylindrically symmetric, so that the x' and y' directions are equivalent and both being perpendicular to the cylinder axis z'. Under this assumption, we choose the x' and y' directions in such form to simplify the transformation from the (x, y, z) frame to that of the (x', y', z') ligand frame.

This transformation matrix generally involves the three Euler angles, but the assumption of cylindrical-ligand symmetry reduces this number to two, as x' and y' are chosen so that the third angle vanishes identically. Thus, the two angles retained are those of the standard transformation from Cartesian to spherical polar coordinates. When this transformation matrix is employed, the $\mu^\beta\mu^\delta$ products occurring in the above equation in the (x, y, z) frame become sums of products in the (x', y', z') frame. Thus, we define [19] the nonvanishing components of the ligand polarizability tensor as follows:

$$\alpha_\parallel = \alpha'_{z'z'} = \sum_{l\neq 0} \frac{2E_l}{E_l^2 - E_a^2} |\mu_{0l}^z|'^2 \tag{12.1}$$

and also

$$\alpha_\perp = \alpha'_{x'x'} = \alpha'_{y'y'} = \sum_{l\neq 0} \frac{2E_l}{E_l^2 - E_a^2} |\mu_{0l}^\perp|'^2, \tag{12.2}$$

where $\perp$ is either x' or y', respectively, and the anisotropic component of the ligand polarizability tensor is given by $\beta\alpha = \alpha_\parallel - \alpha_\perp$.

3.2. Normal coordinate analysis for the $Cr(CN)_6^{3-}$ complex ion in the octahedral point molecular group

In the octahedral point molecular group, the assumed nuclear equilibrium configuration is given in Fig. 1. General and well known symmetry adapted selection rules indicate that the normal modes of vibrations for this system transform as given below [4, 5]

$$\Gamma_{\rm vib} = 2\alpha_{1\rm g} + 2\varepsilon_{\rm g} + \tau_{1\rm g} + 4\tau_{1\rm u} + 2\tau_{2\rm g} + 2\tau_{2\rm u}. \quad (13)$$

The next step in the normal coordinate analysis is to find a complete set of internal coordinates $\boldsymbol{s}$, and then on the basis of symmetry arguments, we obtain the symmetry coordinates by using the well known relation: $\boldsymbol{S} = \boldsymbol{Us}$, where the $\boldsymbol{U}$ matrix is symmetry determined [5]. It is customary in the literature to project the internal coordinates in the nuclear Cartesian basis set, represented by the $\boldsymbol{X}$ matrix, so that the following identity holds: $\boldsymbol{S} = \boldsymbol{Us} = (UB)\boldsymbol{X}$. This identity relates the set of the symmetry coordinates $\boldsymbol{S}$ to the set of the nuclear Cartesian coordinates $\boldsymbol{X}$. The actual details of the calculation can be obtained upon request from R.A.

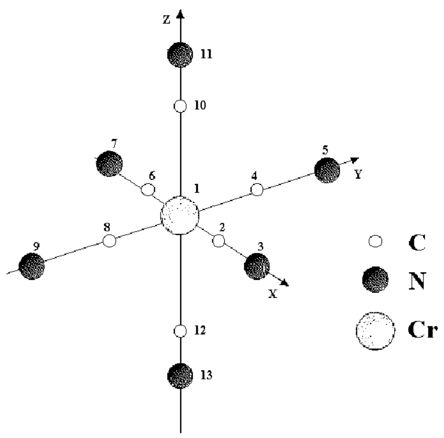

Fig. 1. Nuclear equilibrium configuration.

Also, the symmetry coordinates may be split into three set of coordinates, namely: (a) the framework vibrations (CrC_6), (b) the ligand vibrations (CN) and (c) the ligand-framework coupling vibrations (Cr–C–N). To study, on a semiquantitative basis, the role played by this type of vibrations, we have decided to model the interacting vibrational force field, using several versions. The force fields employed in this calculation are: modified general valence force field (MGVFF), modified Urey–Bradley force field (MUBFF) and resonance interaction valence force field (RIVFF). The details of the normal coordinate analysis can be found in the work by Acevedo and Díaz [5]. The L-matrices (amplitudes of vibrations) connecting the symmetry coordinates to the normal coordinates, by means of the relationship $S = LQ$, depend on the details of the force field employed in the calculation. We have then tabulated the odd parity vibrational frequencies, the L-matrix elements, and the associated potential energy distribution (PED) in Appendix 1.

The normal coordinate analysis was performed assuming an octahedral site symmetry for the Cr^{3+} ions. The Cr–C and C–N bond distances were taken as 1.90 and 1.15 Å, respectively [5]. As MGVFF, MUBFF, and RIVFF are concerned, the symmetrized F matrices are given in Table I, and the calculated force constants in Table II [5]. The number of internal force constants reported in this paper are as follows: MGVFF — 17 , MUBFF — 9 and for the RIVFF — 7, respectively. The calculated internal force constants are as follows: (A) MGVFF: $f_{\rm CrC} = 1.7966$, $f^{t}_{\rm CrC/CrC} = 0.3140$, $f^{c}_{\rm CrC/CrC} = -0.0131$, $f^{c}_{\rm CN/CN} = -0.0810$, $f^{c}_{\rm CN/CN} = -0.0790$, $f_{\rm CN} = 17.0490$, $f_{\beta} = 0.1451$, $f_{\beta\beta'} = 0.0076$, $f_{\beta\beta''} = 0.0202$, $f_{\rm CrC/\alpha} = 0.0252$, $f_{\alpha} = 0.1806$, $f_{\alpha\alpha'} = 0.0248$, $f_{\alpha\alpha''} = 0.0236$, $f_{\alpha\alpha'''} = 0.0036, f_{\alpha\beta} = -0.0175$, $f_{\alpha\beta''} = -0.0049$ and $f_{\alpha\beta'''} = -0.0092$; (B) MUBFF: $K_1({\rm CrC}) = 1.3010$, $K_2({\rm CN}) = 17.001$, $F = 0.0700$, $F' = 0.0600$, $p_1({\rm CrC_1/CrC_2}) = 0.46000$, $p_2({\rm CrC/CN}) = 0.00000$, $H_1(\alpha) = 0.24500$, $H_2(\beta) = 0.11510$ and $p_3({\rm CCrC/CCrC}) = 0.03500$; (C) RIVFF: $F_{\rm CrC} = 1.73100$, $S_{(\rm CrC/CrC)} = 0.31750$, $F_{\rm CN} = 16.86370$, $F_{\beta} = 0.27910$, $P_{(\beta/\beta)} = 0.03560$, $T_{(\alpha/\beta)} = -0.16190$ and $F_{\alpha} = 0.17970$. All these values are given in mdyn/Å.

From the above results and those reported in Appendix 1, it is shown that the MGVFF reproduces rather nicely the observed frequencies and the values for the calculated force constants are reasonable. It is found that the Cr–C stretching force constant (1.80) is smaller than the value for the Co–C (2.10) as reported by Jones [4], in the $Co(CN)_6^{3-}$ion. This is probably due to the smaller degree of π bonding in the $Cr(CN)_6^{3-}$ complex ion. The difference in the electronic structure in the two metals produces an increase in the CN stretching force constant (17.05) in the $Cr(CN)_6^{3-}$ ion, when it is compared with the corresponding value in the $Co(CN)_6^{3-}$ ion (16.77). A careful and detailed discussion may be found in the work of Acevedo et al. [5], and therefore we shall not repeat it here.

3.3. Vibronic intensity calculation

It can be shown that the ${}^2E_{\rm g} \rightarrow {}^4A_{2\rm g}$ transition borrows its intensity mainly from the ${}^4A_{2\rm g} \rightarrow {}^4T_{2\rm g}$ polyelectronic excitation with the explicit cooperation of the odd parity normal modes of vibrations of the complex ion (within the framework of both, a molecular model and the independent system model). This latter electronic transition is made up of three one-electron transitions, namely the $xy \rightarrow x^2 - y^2$ and its cyclic permutations ($x \rightarrow y \rightarrow z \rightarrow x$). A typical matrix element may be written as follows [17, 19, 20]:

$$\langle d_{xy}|D^{k_1}_{q_1}|d_{x^2-y^2}\rangle = -\frac{\mathrm{i}}{2}e\langle r^{k_1}\rangle_{dd}\, c^{k_1}(2+2|2-2)(\delta_{q_1,+4} - \delta_{q_1,-4}), \tag{14}$$

where $k_1 = 4$.

It is interesting to observe that for this particular phosphorescence, the relative vibronic intensity distribution due to the 6 odd parity vibrational modes depends solely on the details of the intramolecular force field. There is no radial dependence on these vibronic intensity ratios, since the expectation values of r^4 between two d-orbital cancels out when the relative vibronic intensity ratios are worked out.

Next, let us define the quantities

$$d_1 = -48\sqrt{2}\alpha_L r_0^{-7}, \qquad d_2 = -48\sqrt{2}\alpha_L(r_0^{-7} + R_0^{-7}),$$

$$d_3 = 48\sqrt{\frac{D}{R_0}}(\alpha_L + \beta\alpha)r_0^{-7}, \qquad d_4 = 48\sqrt{2}(\alpha_L + \beta\alpha)\left[R_0^{-7} + \left(\frac{r_0}{R_0}\right) r_0^{-7}\right],$$

$$d_5 = -d_3 \qquad \text{and} \qquad d_6 = -d_4. \tag{15.1}$$

Here $R_0 = R_0(\text{Cr–C})$, $D = D(\text{C–N})$ and $r_0 = R_0 + D$. The parameter values used in the intensity calculations are as follows: $R_0 = 1.90$ Å, $D = 1.15$ Å, $r_0 = 3.05$ Å, $\alpha_L = 1.21$ Å^3 and $\beta\alpha = 0.6003$ Å^3. Next, when combining Eqs. (11), (12.1), (12.2), (14) and (15.1), it is easy though long and tedious to show that for the one electronic transition $xy \to x^2 - y^2$, the ligand polarization components to the total transition dipole moments may be written as given below

$$\mu^x = -\gamma^{LP}(d_1S_{6b} + d_2S_{7b} + d_3S_{8b} + d_4S_{9b} + d_5S_{12b} + d_6S_{13b}),$$

$$\mu^y = -\gamma^{LP}(-d_1S_{6c} - d_2S_{7c} - d_3S_{8c} - d_4S_{9c} + d_5S_{12c} + d_6S_{13c}),$$

$$\mu^z = 0, \tag{15.2.1}$$

where $\gamma^{LP} = \frac{5}{48}e\langle r^4\rangle_{dd}$ and the set of symmetry coordinates utilized are those listed in Appendix 3. Next, we shall introduce the β_k^{LP} quantities, after using the transformation matrix $S = LQ$, thus relating the set of the symmetry coordinates to the set of the normal coordinates for the system.

Thus we define

$$\beta_6^{LP} = d_1L_{66} + d_2L_{76} + d_3L_{86} + d_4L_{96},$$

$$\beta_7^{LP} = d_1L_{67} + d_2L_{77} + d_3L_{87} + d_4L_{97},$$

$$\beta_8^{LP} = d_1L_{68} + d_2L_{78} + d_3L_{88} + d_4L_{98},$$

$$\beta_9^{LP} = d_1L_{69} + d_2L_{79} + d_3L_{89} + d_4L_{99},$$

$$\beta_{12}^{LP} = d_5L_{12,12} + d_6L_{13,13},$$

$$\beta_{13}^{LP} = d_5L_{12,13} + d_6L_{13,13} \tag{15.2.2}$$

Thus, for the $xy \to x^2 - y^2$, one electron transition, the x, y, and z component of the ligand polarization transition dipole moment become

$$\mu^x = -\gamma^{LP}(\beta_6^{LP}Q_{6b} + \beta_7^{LP}Q_{7b} + \beta_8^{LP}Q_{8b} + \beta_9^{LP}Q_{9b} + \beta_{12}^{LP}Q_{12b}$$
$$+\beta_{13}^{LP}Q_{13b}),$$

$$\mu^y = -\gamma^{LP}(-\beta_6^{LP}Q_{6c} - \beta_7^{LP}Q_{7c} - \beta_8^{LP}Q_{8c} - \beta_9^{LP}Q_{9c} + \beta_{12}^{LP}Q_{12c}$$
$$+\beta_{13}^{LP}Q_{13c}),$$

$$\mu^z = 0. \tag{15.2.3}$$

In terms of the above defined magnitudes, the total ligand polarization dipole strength associated with the $^4A_{2g} \rightarrow {}^4T_{2g}$ polyelectronic transition may be written in a closed form as given below

$$D({}^4A_{2g} \rightarrow {}^4T_{2g}) = 6(\gamma^{LP})^2 \sum_{k=6-13} (\beta_k^{LP})^2 \langle 0|Q_k|1\rangle^2. \tag{16}$$

It is indeed clear that in this order of approximation, the relative vibronic intensity distribution associated with the two excitations, namely the $^2E_g \rightarrow {}^4A_{2g}$ and the intensity source, $^4A_{2g} \rightarrow {}^4T_{2g}$ will be roughly equivalent. This is particularly true since the spin–orbit coupling constant for this complex ion is small, though other than zero. Furthermore, it follows that the relative vibronic intensity distribution of the $^4A_{2g} \rightarrow {}^4T_{2g}$ electronic transition is independent of any radial integral, but is critically dependent upon both the details of the intramolecular force field and the values of the mean and anisotropic ligand polarizability values. We list in Appendix 2 the assignments currently accepted for each and all the normal modes of vibrations for the $Cr(CN)_6^{-3}$ complex ion in the assumed octahedral point molecular group. We also display in Table I the relative vibronic intensity distribution for the sixodd parity vibrational modes and also for the three different force fields employed to model the interacting vibrational force field for this system.

TABLE I

Calculated relative vibronic intensity distributions (the experimental ratios are not available).

Force field	$f(\nu_6)$:$f(\nu_7)$:$f(\nu_8)$: $f(\nu_9)$:$f(\nu_{12})$: $f(\nu_{13})$
MGVFF	1.00 : 1.19 :19.58: 7.58 : 14.69 : 5.58
RIVFF	7.39 : 1.00 :67.07:258.85: 66.06 : 201.78
MUBFF	1.00 : 9.98 : 8.34 : 5.27 : 15.32 : 2.79

TABLE II

Dipole strengths for the $^4A_{2g} \rightarrow {}^4T_{2g}$ transition*.

Oxidation state	MGVFF	RIVFF	MUBFF
+3	2.413×10^{-3}	3.918×10^{-3}	2.076×10^{-3}
+2	6.466×10^{-3}	10.499×10^{-3}	5.564×10^{-3}
+1	23.024×10^{-3}	37.369×10^{-3}	19.802×10^{-3}

*The radial wave functions have been taken from Kibler et al. [21].

We also list in Table II, below the ligand polarization contribution to the total oscillator strength corresponding to the $^4A_{2g} \rightarrow {}^4T_{2g}$ transition for a set of three different central metal ion's oxidation states. This is important, since according to the Gauss theorem, the net charge should be concentrated on the surface of the sphere, and therefore we should expect that an effective charge on the central metal chromium approaches to zero.

It is important to observe that no correction for the refractive index of the medium has been included in the vibronic intensity calculation. Also, the L-matrix corresponding to the various force fields are given in Appendix 4, as well as the calculated potential energy distribution (PED).

4. Discussion

The experimental data referred to the $^2E_g \rightarrow {}^4A_{2g}$ electronic transition indicates that the intensity induced by the normal modes $\nu_8[\tau_{1u} : \delta(\text{Cr–C–N})]$, $\nu_9[\tau_{1u} : \delta(\text{C–Cr–C})]$, $\nu_{12}[\tau_{2u} : \delta(\text{Cr–C–N})]$, $\nu_{13}[\tau_{2u} : \delta(\text{C–Cr–C})]$ should be roughly comparable [1–3]. This experimental finding is reflected by our calculation and as seen from the results given in Table I, the three different force field employed in the calculation give the right pattern for the vibronic intensity distribution (the poorest agreement is achieved by the RIVFF). These results indicate a clear support to our model calculation and are in fairly good agreement with experiment [1–3]. It is also important to analyze the results displayed in Appendix 1, Sec. III. It is shown that for the normal modes associated with the odd parity vibrational frequencies ν_i $(i = 8, 9, 12, 13)$, there is a nonzero coupling among the stretching, bending, and linear bending vibrations and therefore this mixing of the symmetry coordinates should be considered when dealing with the assignments for these types or compounds. We have investigated this mixing of symmetry coordinates, using three different force fields and we can claim that the calculation has been successful, though many limitations and complexity were involved.

There is no doubt that we have proved the importance of the skeletal, the ligand and the framework-ligand vibrations of odd parity in the intensity mechanism associated with this parity forbidden but vibronically allowed electronic transition. There are however several ways of improving the calculation: the obvious one is to take into account the descent of symmetry and also to undertake a full lattice dynamic calculation. All of these improvements are most welcome, however we need fairly accurate data base for these systems.

Acknowledgments

R.A. would like to express his gratitude to Professor W. Stręk and Dr. Barbara Nissen for the friendship and hospitality provided at the Institute for Low Temperature and Structure Research at Wrocław, Poland, where the author spent a wonderful time. Professor C.D. Flint is also acknowledged for valuable comments while M.P. was finishing his Ph.D. at the Chemistry Department, Birkbeck College, University of London. We would also like to thank Drs. Ricardo Letelier (computing evaluation of the polarizability tensor components for the CN fragments) and G. Díaz (normal coordinate analysis for this system). Finally but not at last, both Fondecyt research grant No. 1981207 and grant VRA 2049 from the Universidad Diego Portales are gratefully acknowledged for partial financial support to undertake this research.

Appendix 1

Vibrational frequencies, L-matrix elements, and PED values.

(I) Vibrational frequencies

	Observed	MGVFF	RIVFF	MUBFF
ν_6	2.139	2.139	2.135	2.133
ν_7	467	467	467	480
ν_8	341	341	347	346
ν_9	150	150	143	142
ν_{12}	355	355	347	355
ν_{13}	95	95	103	95

(II) L-matrix elements

(A) MGVFF

		α_{1g}		
CrC	–0.218	0.189		
CN	0.393	0.013		
		ε_g		
CrC	–0.218	0.189		
CN	0.393	0.013		
		τ_{1g}		
CrC	0.688			
		τ_{1u}		
CN	0.393	0.012	0.006	0.001
CrC	–0.221	0.248	0.106	0.016
CrCN	–0.004	0.405	–0.577	0.152
CCrC	–0.008	0.444	–0.303	–0.177
		τ_{2g}		
CrCN	0.668	–0.165		
CCrC	0.555	0.160		
		τ_{2u}		
CrCN	0.676	–0.126		
CCrC	0.385	0.136		

(B) RIVFF

	α_{1g}			
CrC	–0.218	0.189		
CN	0.393	0.013		
	ε_g			
CrC	–0.217	0.190		
CN	0.393	0.010		
	τ_{1g}			
CrC	0.688			
	τ_{1u}			
CN	0.393	0.015	0.000	0.001
CrC	–0.222	0.268	0.005	0.021
CrCN	–0.006	0.157	0.669	–0.217
CCrC	–0.010	0.302	0.297	–0.376
	τ_{2g}			
CrCN	0.687	–0.022		
CCrC	0.509	0.272		
	τ_{2u}			
CrCN	0.668	0.165		
CCrC	0.294	0.283		

(C) MUBFF

	α_{1g}			
CrC	–0.218	0.189		
CN	0.393	0.013		
	ε_g			
CrC	–0.218	0.189		
CN	0.393	0.012		
	τ_{1g}			
CrC	0.688			
	τ_{1u}			
CN	0.393	0.003	0.008	0.001
CrC	–0.218	0.136	0.236	0.005
CrCN	0.000	0.665	–0.207	0.186
CCrC	–0.004	0.543	0.014	–0.161
	τ_{2g}			
CrCN	0.642	–0.248		
CCrC	0.570	0.089		
	τ_{2u}			
CrCN	0.662	–0.187		
CCrC	0.396	0.100		

(III) PED values (note that the values have not been renormalised to unity)

α_{1g}		
$\nu = 2.139$ cm^{-1}	(MGVFF)	$4\nu(\mathrm{CrC}) + 97\nu(\mathrm{CN})$
$\nu = 2.142$ cm^{-1}	(RIVFF)	$4\nu(\mathrm{CrC}) + 96\nu(\mathrm{CN})$
$\nu = 2.150$ cm^{-1}	(MUBFF)	$4\nu(\mathrm{CrC}) + 96\nu(\mathrm{CN})$
$\nu = 360$ cm^{-1}	(MGVFF)	$96\nu(\mathrm{CrC}) + 3\nu(\mathrm{CN})$
$\nu = 360$ cm^{-1}	(RIVFF)	$96\nu(\mathrm{CrC}) + 4\nu(\mathrm{CN})$
$\nu = 358$ cm^{-1}	(MUBFF)	$96\nu(\mathrm{CrC}) + 4\nu(\mathrm{CN})$

ε_{g}		
$\nu = 2.170$ cm^{-1}	(MGVFF)	$3\nu(\mathrm{CrC}) + 97\nu(\mathrm{CN})$
$\nu = 2.135$ cm^{-1}	(RIVFF)	$3\nu(\mathrm{CrC}) + 97\nu(\mathrm{CN})$
$\nu = 2.150$ cm^{-1}	(MUBFF)	$4\nu(\mathrm{CrC}) + 96\nu(\mathrm{CN})$
$\nu = 367$ cm^{-1}	(MGVFF)	$97\nu(\mathrm{CrC}) + 3\nu(\mathrm{CN})$
$\nu = 325$ cm^{-1}	(RIVFF)	$97\nu(\mathrm{CrC}) + 3\nu(\mathrm{CN})$
$\nu = 356$ cm^{-1}	(MUBFF)	$96\nu(\mathrm{CrC}) + 4\nu(\mathrm{CN})$

τ_{1g}		
$\nu = 394$ cm^{-1}	(MGVFF)	$100\delta(\mathrm{CrCN})$
$\nu = 371$ cm^{-1}	(RIVFF)	$100\delta(\mathrm{CrCN})$
$\nu = 346$ cm^{-1}	(MUBFF)	$100\delta(\mathrm{CrCN})$

τ_{1u} symmetry species		
$\nu = 2.139$ cm^{-1}	(MGVFF)	$2\nu(\mathrm{CrC}) + 97\nu(\mathrm{CN})$
$\nu = 2.135$ cm^{-1}	(RIVFF)	$3\nu(\mathrm{CrC}) + 97\nu(\mathrm{CN})$
$\nu = 2.133$ cm^{-1}	(MUBFF)	$2\nu(\mathrm{CrC}) + 97\nu(\mathrm{CN})$
$\nu = 467$ cm^{-1}	(MGVFF)	$67\nu(\mathrm{CrC}) + 10\delta(\mathrm{CrCN}) + 21\delta(\mathrm{CCrC})$
$\nu = 467$ cm^{-1}	(RIVFF)	$3\nu(\mathrm{CN}) + 91\nu(\mathrm{CrC}) - 2\delta(\mathrm{CrCN}) + 9\delta(\mathrm{CCrC})$
$\nu = 480$ cm^{-1}	(MUBFF)	$8\nu(\mathrm{CrC}) + 47\delta(\mathrm{CrCN}) + 45\delta(\mathrm{CCrC})$
$\nu = 341$ cm^{-1}	(MGVFF)	$27\nu(\mathrm{CrC}) + 54\delta(\mathrm{CrCN}) + 17\delta(\mathrm{CCrC})$
$\nu = 347$ cm^{-1}	(RIVFF)	$134\delta(\mathrm{CrCN}) - 34\delta(\mathrm{CCrC})$
$\nu = 346$ cm^{-1}	(MUBFF)	$2\nu(\mathrm{CN}) + 89\nu(\mathrm{CrC}) + 9\delta(\mathrm{CrCN})$
$\nu = 150$ cm^{-1}	(MGVFF)	$4\nu(\mathrm{CrC}) + 34\delta(\mathrm{CrCN}) + 61\delta(\mathrm{CCrC})$
$\nu = 143$ cm^{-1}	(RIVFF)	$6\nu(\mathrm{CrC}) - 31\delta(\mathrm{CrCN}) + 125\delta(\mathrm{CCrC})$
$\nu = 142$ cm^{-1}	(MUBFF)	$43\delta(\mathrm{CrCN}) + 55\delta(\mathrm{CCrC})$

τ_{2g}		
$\nu = 358$ cm^{-1}	(MGVFF)	$54\delta(\mathrm{CrCN}) + 47\delta(\mathrm{CCrC})$
$\nu = 406$ cm^{-1}	(RIVFF)	$94\delta(\mathrm{CrCN}) - 5\delta(\mathrm{CCrC})$
$\nu = 440$ cm^{-1}	(MUBFF)	$29\delta(\mathrm{CrCN}) + 71\delta(\mathrm{CCrC})$
$\nu = 117$ cm^{-1}	(MGVFF)	$46\delta(\mathrm{CrCN}) + 53\delta(\mathrm{CCrC})$
$\nu = 183$ cm^{-1}	(RIVFF)	$5\delta(\mathrm{CrCN}) + 94\delta(\mathrm{CCrC})$
$\nu = 108$ cm^{-1}	(MUBFF)	$71\delta(\mathrm{CrCN}) + 29\delta(\mathrm{CCrC})$

	τ_{2u}	
$\nu = 355$ cm^{-1}	(MGVFF)	$65\delta(\mathrm{CrCN}) + 33\delta(\mathrm{CCrC})$
$\nu = 347$ cm^{-1}	(RIVFF)	$134\delta(\mathrm{CrCN}) - 34\delta(\mathrm{CCrC})$
$\nu = 355$ cm^{-1}	(MUBFF)	$47\delta(\mathrm{CrCN}) + 52\delta(\mathrm{CCrC})$
$v = 95$ cm^{-1}	(MGVFF)	$34\delta(\mathrm{CrCN}) + 66\delta(\mathrm{CCrC})$
$\nu = 103$ cm^{-1}	(RIVFF)	$-34\delta(\mathrm{CrCN}) + 134\delta(\mathrm{CCrC})$
$\nu = 95$ cm^{-1}	(MUBFF)	$52\delta(\mathrm{CrCN}) + 47\delta(\mathrm{CCrC})$

Appendix 2

Modes of vibrations for the thirteen-atom systems.

α_{1g}	ν_1	$\nu(\mathrm{CrC})$
	ν_2	$\nu(\mathrm{CN})$
ε_g	ν_3	$\nu(\mathrm{CrC})$
	ν_4	$\nu(\mathrm{CN})$
τ_{1g}	ν_5	$\delta(\mathrm{CrCN})$
τ_{1u}	ν_6	$\nu(\mathrm{CN})$
	ν_7	$\nu(\mathrm{CrC})$
	ν_8	$\delta(\mathrm{CrCN})$
	ν_9	$\delta(\mathrm{CCrC})$
τ_{2g}	ν_{10}	$\delta(\mathrm{CrCN})$
	ν_{11}	$\delta(\mathrm{CCrC})$
τ_{2u}	ν_{12}	$\delta(\mathrm{CrCN})$
	ν_{13}	$\delta(\mathrm{CCrC})$

References

[1] C.D. Flint, P. Greenough, *J. Chem. Soc. Faraday Trans. II* **70,** 815 (1974).

[2] C.D. Flint, P. Greenough, *Chem. Commun.* **1,** 489 (1973).

[3] C.D. Flint, *Chem. Phys. Lett.* **2,** 661 (1968).

[4] L.R. Jones, R.S. McDowell, M. Goldblatt, *Inorg. Chem.* **8,** 2349 (1969); I. Nakagawa, T. Shimanouchi, *Spectrochimica Acta* **18,** 101 (1962); L.H. Jones, *J. Mol. Spectrosc.* **8,** 105 (1962).

[5] R. Acevedo, G. Díaz, *Spectrosc. Lett.* **19,** 73 (1986).

[6] V. Barkhatov, H. Zhdanov, *Acta Physicochim. (URSS)* **16,** 43 (1942).

[7] V. Barkhatov, *Acta Physicochim. (URSS)* **16,** 123 (1942).

[8] N.A. Curry, W.A. Runciman, *Acta Crystallogr.* **12,** 647 (1959).

[9] J.O. Artman, J.C. Murphy, J.A. Kohn, W.D. Townes, *Phys. Rev. Lett.* **4,** 607 (1960); J.A. Kohn, W.D. Townes, *Acta Crystallogr.* **14,** 617 (1961).

[10] L.H. Jones, *J. Chem. Phys.* **36,** 1209 (1962).

[11] J.R. Partington, *An Advanced Treatise of Physical Chemistry*, Vol. 4, Longmans, Green Co., London 1953, p. 42.

[12] A.I. Vogel, *J. Chem. Soc.* **1,** 1833 (1948).

[13] K.G. Denbigh, *Trans. Faraday Soc.* **36,** 936 (1940).

[14] C.G. LeFebre, R.J.W. Lefrere, *Rev. Pure Appl. Chem.* **5,** 261 (1955).

[15] J.A. Applequist, J.R. Carl, K.K. Fung, *J. Am. Chem. Soc.* **94,** 2959 (1972).

[16] N.J. Bridge, A.-D. Buckingham, *Proc. R. Soc. London A* **259,** 334 (1966).

[17] R. Acevedo, in: *Vibronic Processes in Inorganic Chemistry*, Ed. C.D. Flint, *NATO-ASI Series C: Mathematical and Physical Sciences*, Vol. 288, Kluwer Academic, 1989, p. 139.

[18] C.J. Ballhausen, in Ref. [17], p. 1.

[19] R. Acevedo, S.O. Vásquez, C.D. Flint, *Theor. Chim. Acta (Berlin)* **73,** 349 (1991).

[20] R. Acevedo, S.O. Vásquez, C.D. Flint, *Mol. Phys.* **74,** 843, 853 (1991).

[21] F.M.O. Michel-Calendini, M.R. Kibler, *Theor. Chim. Acta (Berlin)* **10,** 367 (1968).

[22] R. Acevedo, S.O. Vásquez, M. Passman, *An. Quím.* **90,** 237 (1994).

[23] R. Acevedo, T. Meruane, E. Cortés, V. Poblete, *An. Quím.* **91,** 479 (1995).

[24] R. Acevedo, S.O. Vásquez, *An. Quím.* **91,** 526 (1995).

[25] R. Acevedo, C.D. Flint, T. Meruane, G. Muñoz, M. Passman, V. Poblete, *J. Mol. Struct. (Theochem.)* **390,** 109 (1997).

[26] R. Acevedo, Ph.D. thesis, University of London, 1981.

[27] W. Stręk, J. Sztucki, *Chem. Phys. Lett.* **177,** 407 (1991).

[28] M.T. Berry, A.F. Kirby, F.S. Richardson, *Mol. Phys.* **66,** 723 (1989).

[29] P. Caro, O.K. Moune, E. Antic-Fidancev, M. Lemaitre-Blaise, *J. Less-Common Met.* **112,** 153 (1985).

[30] T. Meruane, R. Acevedo, *Theor. Chim. Acta (Berlin)* **62,** 30 (1983).